Effects of Neonatal Freeze Lesions on Expression of Parvalbumin in Rat Neocortex

Glenn D. Rosen, Kimberle M. Jacobs[1] and David A. Prince[1]

Dyslexia Research Laboratory and Charles A. Dana Research Institute, Beth Israel Deaconess Medical Center, Division of Behavioral Neurology, Beth Israel Deaconess Medical Center, 330 Brookline Avenue, Boston MA 02215, Harvard Medical School, Boston, MA 02115 and [1]Department of Neurology and Neurological Sciences, Stanford University Medical Center, Stanford, CA 94305-5300, USA

Neonatal freeze lesions to the cortical plate result in focal malformations of the cerebral cortex that resemble four-layered microgyria. These malformations have been associated with local and distant changes in neuronal architecture, and have been implicated in the neocortical epileptiform discharges that can spread up to 4 mm away from the malformation itself. In an effort to assess potential changes in the development of one population of inhibitory interneurons in this malformation, we measured the density of parvalbumin-immunoreactive (ParvIR) neurons in microgyric and control cerebral cortex on postnatal days 13, 15, 21 and 64. In comparison to controls, microgyric animals exhibited a transient decrease in the expression of parvalbumin immunoreactivity in supragranular neurons, both within the malformation itself and in normal six-layered cortex up to 2 mm adjacent to it. This difference disappeared by P21. In addition, there was a permanent diminution of the density of ParvIR neurons in infragranular layers both within and immediately adjacent to the microgyrus. These results indicate that early injury to the cortical plate gives rise to both focal and more widespread changes in cortical architecture.

Introduction

Cortical malformations induced in rodents by injury to the cortical plate during neuronal migration provide a model for study of disorders such as dyslexia and epilepsy. A malformation resembling four-layered microgyria is produced by hypoxic/ischemic damage to the developing cortical plate following either cold injury (Dvorák and Feit, 1977; Dvorák *et al.*, 1978; Humphreys *et al.*, 1991; Suzuki and Choi, 1991; Rosen *et al.*, 1992; Ferrer *et al.*, 1993; Jacobs *et al.*, 1996a; Luhmann and Raabe, 1996) or ibotenic acid injections (Innocenti and Berbel, 1991a; Marret *et al.*, 1995) during the period of late neuronal migration.

The anatomical and physiological consequences of focal freeze lesions are seen not only locally within the damaged cortex, but also in regions outside of the malformation. Glutamatergic fibers are nearly absent in the microgyric region but are present and disorganized in adjacent cortex, which appears in Nissl stains to be unaffected (Humphreys *et al.*, 1991). This region adjacent to the microgyrus has also been shown to be epileptogenic (Jacobs *et al.*, 1996a; Luhmann and Raabe, 1996). Epileptiform discharges evoked within this paramicrogyral zone spread as much as 2–4 mm from the site of stimulation (Jacobs *et al.*, 1996a; Luhmann and Raabe, 1996). Recent findings have suggested hemisphere-wide changes in the levels of excitatory and inhibitory receptor binding. Specifically, AMPA, kainate and NMDA receptors are up-regulated, while both γ-aminobutyric acid-A ($GABA_A$) and $GABA_B$ receptors are down-regulated throughout the cerebral cortex ipsilateral to the cortical lesion (Luhmann *et al.*, 1997). Finally, evidence suggests that this focal malformation can alter behavior as well. Microgyric male rats (but not females) have difficulty performing a fast auditory discrimination task (Fitch *et al.*, 1994, 1997), and this difference is reflected in the distribution of neuronal sizes in the medial geniculate nuclei of these animals (Herman *et al.*, 1997).

Jacobs *et al.* (1996a) recently reported a near absence of parvalbumin-like immunoreactive cells in microgyria induced by freeze injury. A decrease of these cells in other induced malformations of rodent cortex, and in focal cortical regions from an epilepsy patient, has also been described (Ferrer *et al.*, 1992, 1993). However, gross examination of the density of parvalbumin-immunoreactive (ParvIR) neurons in tissue from adult microgyric rats did not show any obvious decrease (unpublished observations). Because the results reported by Jacobs *et al.* (1996a) were from immature animals, the possibility existed that there might be age-related differences in parvalbumin expression in the microgyric rats. In the current study we qualitatively and quantitatively examined this question with tissue taken from two laboratories at three different ages. We hypothesized that there was a temporary down-regulation of parvalbumin expression in malformations induced by freeze injury. In addition, we sought to determine whether there were any transient or long-term changes in parvalbumin expression in regions outside of the microgyrus.

Materials and Methods

The data presented here were collected from a series of brains prepared in laboratories at Beth Israel Deaconess Medical Center (BIDMC) and Stanford University Medical Center (SUMC). Although the histological and histochemical procedures differed slightly between the two groups, *post-hoc* analysis (see Results) showed no difference in the data derived from the two laboratories. As the majority of the methods have been described in detail elsewhere, they are only outlined briefly here with the small differences in techniques noted when appropriate.

Induction of Freeze Injury

BIDMC

Microgyria were induced by a modification of the technique of Dvorák and colleagues (Dvorák and Feit, 1977; Dvorák *et al.*, 1978), reported in detail elsewhere (Humphreys *et al.*, 1991; Rosen *et al.*, 1992). Pregnant Wistar rats were obtained from Charles River (Wilmington, MA) and on the day after birth (P1), their pups were anesthetized with hypothermia, and a small anteroposterior incision was made in the scalp over the left hemisphere, exposing the skull. A cooled (–70°C) 2 mm diameter stainless steel probe was placed on the skull ~2 mm lateral of the sagittal suture and 2 mm caudal of bregma for either 2, 5, 10 or 20 s. Animals receiving sham surgery were treated identically to those receiving a freeze injury except that the probe was maintained at room temperature. After surgery, the scalp was quickly sutured, subjects marked with ink injections to the footpads, warmed under a lamp and returned to the dam.

SUMC

Microgyria were induced as above, with the following variations: Sprague–Dawley rats were used. Pups were given freeze lesions on either P0 or P1. A copper probe with a rectangular shaped tip (2 × 5 mm),

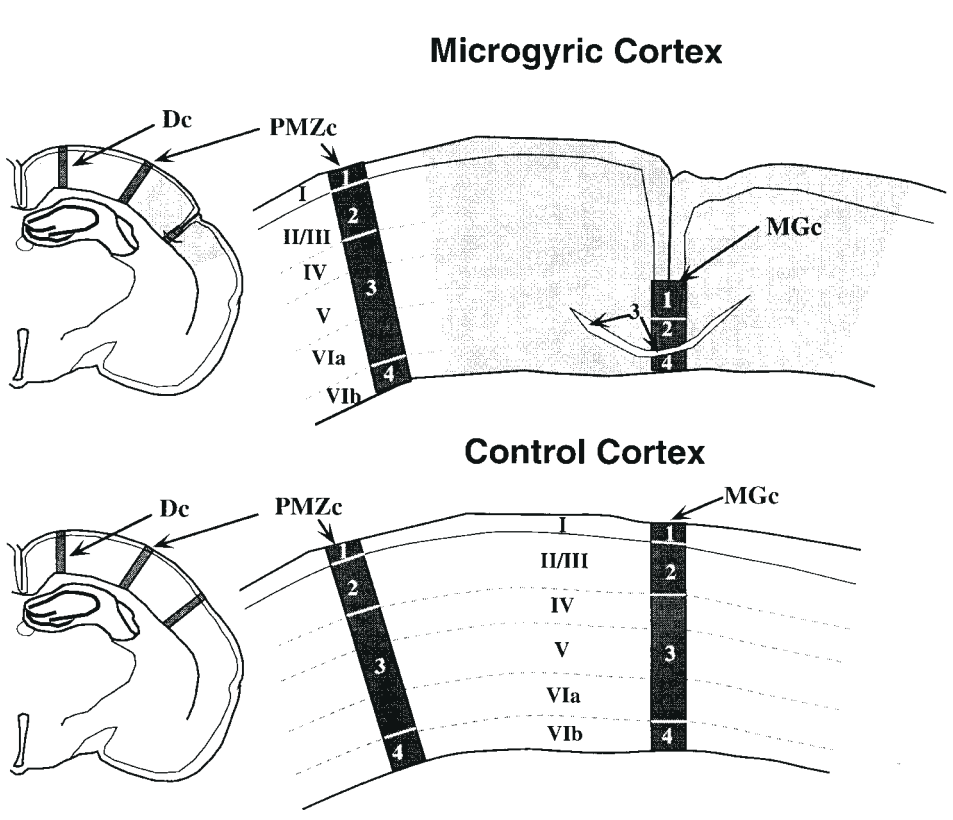

Figure 1. Schematic diagram illustrating methodology of ParvIR neuron counting. The section containing the microgyric, four-layered region (gray area) is matched to that of a control section. Columns in insets on left show sites within microgyric and control cortex from which counts were obtained. MGc, microgyria column underneath the center of the microgyrus, usually under the microsulcus; PMZc, paramicrogyral zone column, 200 μm outside the border of the microgyrus; Dc, distant column, 2000 μm from the border of the microgyrus. ParvIR neurons were counted as described in the text. Uppercase Roman numerals: laminae of normal six-layered cortex. Lowercase Roman numerals: laminae of four-layered microgyric cortex. Arabic numerals: strata of counting columns. Stratum 1, microgyric layer i or normal layer I; stratum 2, microgyric layer ii or normal layer II/III; stratum 3, microgyric layer iii or normal layers IV, V and VIa; stratum 4, microgyric layer iv or normal layer VIb.

cooled with isobutane in dry ice, was placed on the skull for 3–7 s. Controls were naïve littermates of the same age.

Histology

BIDMC. On P15, P21 or P64, the animals were anesthetized (pentobarbital 60 mg/kg) and perfused transcardially with 0.9% saline followed by 4% paraformaldehyde. The brains were removed and post-fixed for 24 h, cryoprotected with sucrose buffer, frozen on dry ice, serially sectioned in the coronal plane at 40 μm, and sections stored in 0.1 M sodium phosphate buffer. Every tenth section was stained with Thionin for Nissl substance and adjacent sections were reacted for parvalbumin (see below).

The numbers of animals generated were as follows: P15 — four lesioned, one control; P21 — six lesioned, two control; P64 — eight lesioned, one control.

SUMC. Procedures were as above, with the following differences. After perfusion and immersion fixation in 4% paraformaldehyde overnight, 40 μm coronal sections were cut with a vibratome. A naïve sibling brain was processed simultaneously with every freeze-lesioned brain. Every third section was taken for parvalbumin staining, with adjacent sections stained for Nissl. Eight P13 rats with sibling controls were used.

Nissl. Mounted sections were stained for Nissl substance with 0.05% Thionin using standard techniques.

Parvalbumin Immunohistochemistry

BIDMC. Free-floating sections were rinsed twice in phosphate-buffered saline (PBS, pH 7.4) for 5 min each and transferred to a buffered 0.6% hydrogen peroxide solution in order to block staining of endogenous peroxidases. The sections were then rinsed twice in PBS and incubated overnight at 4°C in a 1/2500 dilution of mouse anti-parvalbumin immunoglobulin (ICN, Lisle, IL). The vehicle (diluent) for all antibody incubations was 3% rabbit serum in PBS with 0.3% Triton X-100.

Sections were then placed into a solution containing the linking antibody [rabbit anti-mouse immunoglobulin; Dakopatts (Santa Barbara, CA) Z259 — diluted 1/20] at room temperature for 2 h. The sections were rinsed twice with PBS and placed in a 1/250 dilution of mouse peroxidase anti-peroxidase (Dakopatts B650) at room temperature for 2 h. The tissue was rinsed twice in PBS, twice in 50 mM Tris buffer (pH 7.6), and developed using 0.05% diaminobenzidine and 0.005% hydrogen peroxide diluted in Tris. After rinsing with Tris, sections were mounted on chrome-alum coated slides, dehydrated, counterstained with methyl green/alcian blue, and coverslipped with Permount.

SUMC. Free-floating sections were processed as previously described (Jacobs *et al.*, 1996a). Experimental and control sections from the same anterior–posterior (a–p) level were placed in the same well. The rabbit anti-mouse muscle parvalbumin was kindly supplied by Dr K.G. Baimbridge. A standard ABC kit (Vector Labs) was used to visualize the antibody. Sections were mounted on gelatin-coated slides, dehydrated and coverslipped with Permount.

Quantitative Analysis

All analyses were performed at BIDMC and sections from both BIDMC and SUMC were treated identically. A primary observer (G.D.R.) measured all the sections and a secondary observer (K.M.J.) measured a subset of these (four experimental and three control), sampling from all ages and from tissue processed in both locations. For each lesioned subject in the study, measurements were taken from one experimental section representing the a–p center of the lesion, and one control section matched to the same a–p level.

ParvIR neurons were measured using a computer-assisted methodology (Williams and Rakic, 1988). We counted the number of ParvIR neurons in three 200 μm columns in both the microgyric and control animals, as shown in Figure 1. The microgyric column (MGc) was in the (medial-lateral) center of the microgyric cortex. The paramicrogyral zone column (PMZc) was 200 μm outside the border of the microgyric region, and the distal column (Dc) was located 2 mm away from the PMZc in the direction away from the microgyrus. PMZc and Dc were placed either medial or lateral to MGc depending on the location of the microgyrus, so that Dc would lie within the neocortex of the lesioned hemisphere, and not in either entorhinal cortex laterally or past the midline medially. For the matched control sections, each of the counting columns were placed precisely in the region homologous to that counted in the microgyric subjects, by overlaying control and experimental sections.

Images were taken at 200× on a Zeiss Universal microscope (Carl Zeiss, Inc., Thornwood, NY), and projected onto a Sony GVM 1310 monitor (Sony Corporation, Park Ridge, NJ) connected to an Apple Macintosh Centris 650 workstation (Apple Computer, Cupertino, CA). A counting rectangle (CR; 200 × 250 μm) was overlaid on these images with the top of the CR aligned with the pial surface. On a digitizing tablet, ParvIR neurons were traced, with neurons touching the bottom and right side of the CR being omitted. The software kept track of both the number of neurons and their location (*X* and *Y* coordinates) in the CR. When all ParvIR neurons in the first CR were counted, the slide was moved such that the portion of the slide that was touching the bottom of the previous counting rectangle was now touching the top. An indication that neurons in the second CR were being counted was then made within the data file. The ParvIR neurons were then counted in this CR as described above, and the procedure was repeated for each CR until the layer VIb/white matter border was reached. The *Y* coordinate for this border was noted.

After measurement of the parvalbumin-stained material was completed, the adjacent Nissl-stained section was examined under the same magnification for the purpose of determining laminar borders. For MGc, the CR was placed in precisely the same area as MGc of the parvalbumin-stained section, and fixed so that its top was aligned with the pial surface. The *Y* coordinate for each laminar border was then determined using the software as described above. For example, if the layer IV–V border was determined to be in the fourth counting box with a *Y* coordinate of 100, then the distance from the pial surface would be 850 μm – three full CRs (750 μm) plus 100 μm. From this measure, it was possible to normalize for total depth of the cortex at each counting site and express laminar borders as a percentage of cortical depth. Using the example above, if the total cortical depth was 1800 μm, then the layer IV–V border would be at 47.22% of the depth of cortex. The *Y* coordinates of the ParvIR neurons were then normalized in the same manner. In order to control for relative changes in the size of various lamina, a measure of ParvIR neurons was computed over a fixed laminar distance by dividing the number of ParvIR neurons by the actual thickness (in μm) of the layer containing the neurons. This measure provides an indication of the relative density of ParvIR neurons within a given lamina and is expressed as ParvIR/20 000 μm^2.

One obvious difficulty is the comparison of information from four-layered microgyric cortex to that of six-layered cortex (e.g. Fig. 2). Previous research had shown that mostly late-generated neurons comprise layer ii of the microgyrus and that the birthdates of these neurons correspond with those of layers II/III in normal cortex (Dvorák *et al.*, 1978; Suzuki and Choi, 1991; Rosen *et al.*, 1996). Further, it is evident that at the time of the freeze lesions, nearly all the neurons in the cortical plate underlying the freezing probe (layers IV–VIa) are destroyed, and that this necrotic region resolves into layer iii of the microgyrus, the so-called lamina dissecans (Dvorák and Feit, 1977). Often, but not always, layer VIb escapes damage from the freezing lesion and comprises layer iv of the malformation (Dvorák and Feit, 1977). With this information in mind, we matched data from four-layered microgyric cortex to six-layered normal cortex as follows: stratum 1 = microgyric layer i and normal layer I; stratum 2 = microgyric layer ii and normal layer II/III; stratum 3 = microgyric layer iii and normal layers IV, V and VIa; stratum 4 = microgyric layer iv and normal layer VIb (Fig. 1).

Data were analyzed by repeated-measures ANOVA and Pearson product–moment correlations.

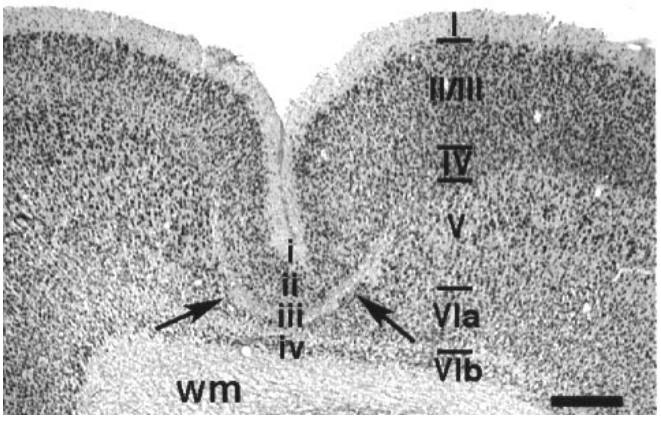

Figure 2. Photomicrograph of Nissl-stained section from cerebral cortex of a P64 rat illustrating typical microgyrus. In comparison to typical six-layered normal cortex (uppercase Roman numerals), the microgyric region contains four layers (lowercase Roman numerals). Arrows delineate the lamina dissecans (layer iii) of the microgyrus. Scale bar 400 = μm. wm, white matter.

Results

Qualitative Analysis

Freeze injury to the developing cortical plate resulted in a malformation resembling four-layered microgyria (Fig. 2). These malformations were located in the architectonic regions HL, FL, Par1, Par2 and Oc1 (Zilles, 1985), and were rarely restricted to one region. More typically, these lesions would traverse borders between two or more architectonic areas (Fig. 3). Comparison of lesioned brains with controls matched for architectonic location controlled for these differences. For the BIDMC brains there were variations in the severity of the lesion which were related to the amount of time that the freezing probe was applied to the skull (2–20 s). Increases in the duration of the freeze lesion were usually associated with deeper microsulci and/or the formation of multiple microsulci. The microgyria generated at SUMC were structurally similar to those generated with 5 s lesions at BIDMC; typically a single microsulcus was surrounded by ~600 μm of four-layered cortex. These differences in the sizes of the microgyri did not affect the overall findings, since the counting column was always located either at the center of the four-layered region or at a specified distance from the clearly identifiable border of the microgyrus.

Examination of the brains of rats killed at P13 or P15 (n = 12) supported previous observations (Jacobs *et al.*, 1996a) that there was a gross decrease in the numbers of ParvIR neurons in the microgyric cortex as compared to adjacent six-layered cortex, as well as compared to control cortex (Fig. 3*A–D*). This was true for tissue generated at both BIDMC and SUMC. In contrast, by P21 (n = 8) there was no obvious difference in the density of ParvIR between layer ii of the microgyria and layer II/III of adjacent, undamaged cortex or compared to layer II/III of controls (Fig. 3*E–G*). These differences in ParvIR at P13–15 were present despite the fact that there was little change in the gross appearance and laminar composition of the microgyria between P13-P15 and P21 (see Fig. 3*A*,*E*). The laminar pattern of ParvIR staining normally develops from an immature to a mature pattern during the second week of life (Sanchez *et al.*, 1992; Soriano *et al.*, 1992). These changes include increases in the overall number of ParvIR neurons and density of ParvIR neuropil staining, and a change from a single dense band of neuropil

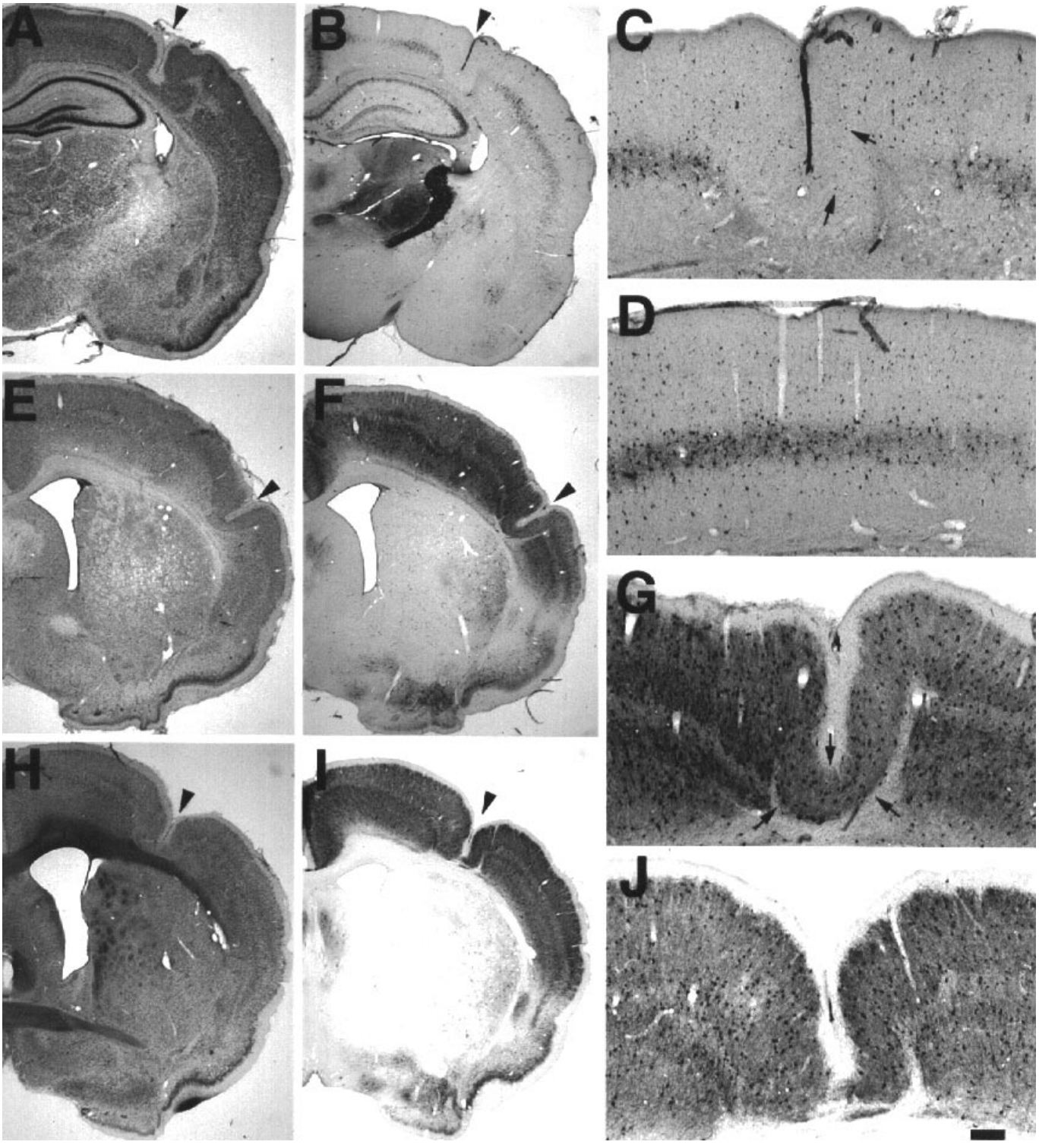

Figure 3. (*A–D*) Photomicrographs from a P15 rat that received a freeze lesion on P1. Nissl-stained (*A*) and adjacent Parvalbumin-stained (*B*) sections from the left hemisphere. Arrowheads denote microsulcus. Higher power photomicrograph (*C*) illustrating the relative decrease of ParvIR neurons in layer ii of the microgyrus (arrows denote ParvIR neurons) when compared to homologous region from a control brains (*D*). (*E–G*) Photomicrographs of cortical sections from a P21 rat that received a freeze lesion on P1. Nissl-stained (*E*) and adjacent parvalbumin-stained (*F*) sections from the left hemisphere. Arrowheads denote microsulcus. Higher power photomicrograph (*G*) illustrating no obvious change in the number of ParvIR neurons in layer ii of the microgyrus (arrows in *G*) compared to adjacent, undamaged cortex. (*H–J*) Photomicrographs of cortical sections from a P64 rat that received a freeze lesion on P1. Nissl-stained (*H*) and adjacent parvalbumin-stained (*I*) sections from the left hemisphere. Arrowheads denote microsulcus. Higher power photomicrograph (*J*) illustrating no obvious change in the number of ParvIR cells in layer ii of the microgyrus when compared to adjacent, six-layered cortex. Bar (in *J*) for *A*, *B*, *E*, *F*, *H*, *I* = 800 μm; for *C*, *D*, *G*, *J* = 200 μm.

Table 1
Mean ± SEM ParvIR neurons/20 000 μm^2 for strata 1 and 4 of Young (≤P15) and Old (≥P21) Lesioned and Control rats. There are no significant differences in either of these layers.

Groups	MGc	PMZc	Dc
Stratum 1			
Young Lesion	0.17 ± 0.08	0.11 ± 0.07	0.00 ± 0.00
Young Control	0.12 ± 0.08	0.05 ± 0.05	0.07 ± 0.07
Old Lesion	0.15 ± 0.07	0.39 ± 0.18	0.35 ± 0.14
Old Control	0.24 ± 0.12	0.13 ± 0.09	0.19 ± 0.14
Stratum 4			
Young Lesion	0.57 ± 0.26	0.34 ± 0.20	0.36 ± 0.22
Young Control	0.29 ± 0.17	0.72 ± 0.55	0.69 ± 0.30
Old Lesion	0.50 ± 0.23	0.61 ± 0.28	0.59 ± 0.25
Old Control	1.08 ± 0.37	0.85 ± 0.46	0.76 ± 0.22

staining within layer V to two bands of intense ParvIR neuropil, within layers IV and Vb respectively (see Fig. 3). This developmental change in the laminar pattern was seen in cortex adjacent to the microgyrus, in contralateral cortex and in control cortex, so that there was a general increase of all ParvIR neurons throughout the neocortex in the P21 animals compared to the earlier ages. In P64 rats (n = 6), there was again no obvious difference in the density of ParvIR neurons in layer ii of the microgyrus as compared to layers II/III of adjacent six-layered cortex (Fig. 3*H–J*), contralateral cortex, or cortex of control animals.

Quantitative Analysis

Preliminary Analysis

Interobserver Reliability. There were seven brains (four experimental, three control) that were measured by two observers. Both observers were blind as to the results of the other's measures. A repeated-measures ANOVA used to determine the total-test reliability (Denenberg, 1979) yielded an r_{tt} of 0.942, which was significant (P < 0.001). A Pearson product–moment correlation also showed significant agreement between the two observers (r = 0.868, P < 0.001). These results support the reliability of the dependent measures.

Inter-laboratory Differences. In order to test for any differences in the dependent measures between the two laboratories, a comparison was made between the P13 subjects from SUMC and P15 subjects of BIDMC (the only age where tissue from both laboratories was quantitatively analyzed). A series of two-way ANOVAs were performed with Location (BIDMC versus SUMC) and Experimental Group (Lesion versus Control) as the independent measures, and the number of ParvIR neurons and the density of ParvIR neurons within each strata for each column as dependent measures. There were no significant Location effects for any variable (P > 0.05 in all cases). Thus, despite different antibodies and slightly different lesioning and sectioning techniques, there were no differences between the values derived from tissue from the different locations. For further analysis, location was therefore ignored.

Differences between P21 and P64 Animals. Because qualitative analysis suggested that there were no differences in ParvIR between P21 and P64 animals, we performed a series of repeated-measures ANOVAs in order to determine whether there were any quantitative differences between these two ages. In this analysis Age (P21 versus P64) was a between measure, and Column (MGc, PMZc, Dc) and Lesion (Lesioned versus Control) were the within measures, with ParvIR/20 000 μm^2 as the dependent measure. ANOVAs were computed separately for each of the four strata. There were no significant interactive effects of Age with any of the other variables, so the subjects from P21 and P64 were pooled together as the 'Old' age group in the quantitative analyses described below.

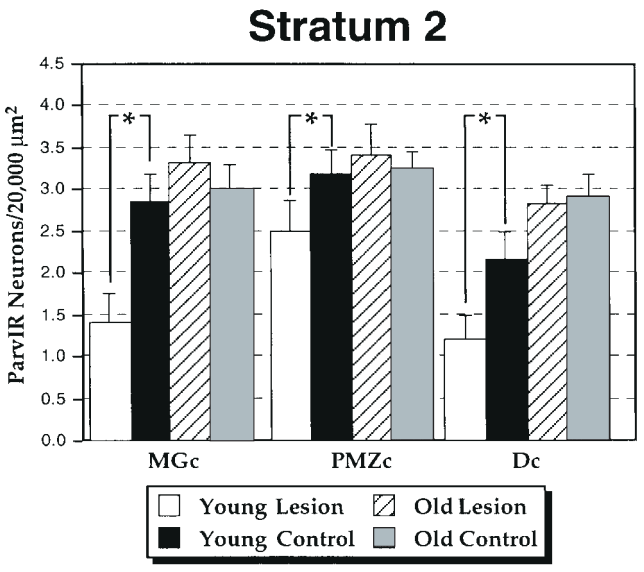

Figure 4. Summary of quantitative data for stratum 2. Bar graphs show the density of ParvIR neurons/20 000 μm^2 (± SEM) in microgyric and control rats. 'Young' rats were killed at ≤P15 and 'Old' rats at ≥P21. *Statistically significant difference (P < 0.05).

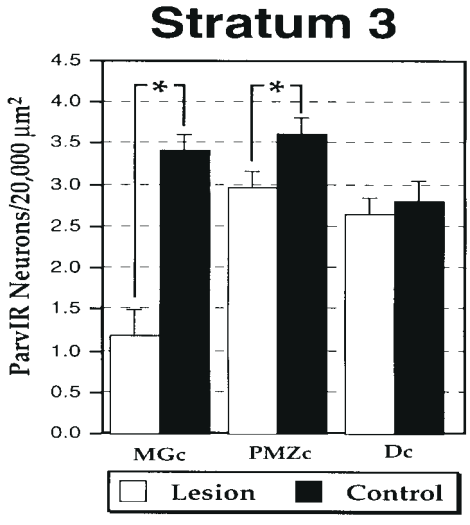

Figure 5. Summary of quantitative data for stratum 3. Bar graphs show the density of ParvIR neurons/20 000 μm^2 (± SEM) in microgyric and control rats. There were no differences between young and old rats, so their data are pooled. *Statistically significant difference (P < 0.05).

Analysis of ParvIR neuronal density

From qualitative observations it was hypothesized that there would be a significant difference in ParvIR neurons/unit area for stratum 2 of the microgyrus compared to stratum 2 of control cortex in the P13-P15 ('Young') group, and that this difference would not be apparent in the older animals. In order to test this

hypothesis, a series of two-within, one-between repeated-measures ANOVAs were computed for the number of ParvIR neurons for each of the strata. In these ANOVAs, Age (Young versus Old) was the between variable with Column (MGc, PMZc, Dc) and Lesion (Lesion versus Control) as the within variables and ParvIR/20 000 μm^2 as the dependent measure. Strata 1 (the molecular layer for both lesioned and control animals) and 4 contained very few ParvIR neurons and no significant differences between any groups were found (see Table 1). The results of these analyses are summarized in Figure 4 for stratum 2 and Figure 5 for stratum 3.

Stratum 2. Overall, there was a significant effect of Age [$F(1,24) = 9.23$, $P < 0.01$], Lesion [$F(1,24) = 10.75$ $P < 0.001$], and the interaction of these two variables [$F(1,24) = 17.63$, $P < 0.001$]. These results indicated that there was a greater concentration of ParvIR neurons in older animals in general, and that there was a significant difference between lesioned and control animals in the youngest age group (≤P15), but there was no such difference in the older animals (≥P21). Examination of the data from the individual Columns shows that this pattern holds for all Columns (Fig. 4). There was a significant effect of Column [$F(2,48) = 10.37$, $P < 0.001$], indicating an overall greater density of cells in PMZc than in either MGc or Dc.

Stratum 3. We expected to see significant differences between lesion and control groups in layer 3 for MGc at all ages, since this is the region in which neurons are killed in the freeze-lesioned animals. The overall ANOVA revealed a significant effect of Column [$F(2,48) = 18.32$, $P < 0.001$], Lesion [$F(1,24) = 26.53$, $P < 0.001$], and the interaction between these two variables [$F(2,48) = 28.23$, $P < 0.001$]. Further examination showed that there were in fact fewer ParvIR neurons in the lesioned animals relative to controls in MGc [$F(1,24) = 42.66$, $P < 0.001$] and PMZc [$F(1,24) = 9.98$, $P < 0.01$], but not in Dc [$F(1,24) = 1.04$, NS]. The findings in PMZc were unexpected, since that column is comprised of six-layered cortex outside of the microgyrus. These results suggest that there is a long-term decrease in expression of infragranular neuronal ParvIR in cortex immediately adjacent to microgyric regions, but not in distant cortex (Fig. 5).

In order to determine which of the laminæ contributed most to this decrease in stratum 3, the density of ParvIR neurons from the constituent layers comprising this stratum (layers IV, V and VIa) were evaluated for the PMZc. There was a significant decrease in the density of ParvIR neurons in lesioned as compared to control animals in layer IV [$F(1,24) = 5.03$, $P < 0.05$], and layer V [$F(1,24) = 9.02$, $P < 0.01$], but not layer VIa [$F(1,24) < 1$, NS]. These results are illustrated in Figure 6.

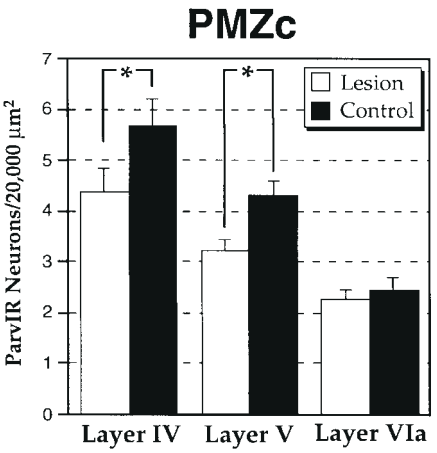

Figure 6. Density of ParvIR neurons/20 000 μm^2 (± SEM) from stratum 3 of paramicrogyral zone column (PMZc), showing numbers in layers IV, V and VIa. *Statistically significant difference ($P < 0.05$).

Discussion

These results demonstrate that the density of ParvIR neurons is low throughout most of neocortex ipsilateral to a microgyrus in immature rats, and that this decrease of expression of parvalbumin immunoreactivity persists in older animals only within layers IV and V immediately adjacent to the microgyrus. The findings will be considered in light of what is known about the ontogeny and modulation of parvalbumin immunoreactivity and other GABAergic markers in the cortex.

Control Tissue

The calcium-binding protein parvalbumin is expressed in subclasses of interneurons, and nearly 100% of these cells co-express GABA (Ren *et al.*, 1992). In the developing cerebral cortex, ParvIR neurons are not seen until the end of the first postnatal week (Solbach and Celio, 1991; Soriano *et al.*, 1992); however, by P12 they are present in all cortical laminæ except layer I, and their distribution achieves a mature pattern by P21 (Soriano *et al.*, 1992). Examination of our control tissue confirms these findings. Specifically, we have seen a remarkable progression in the intensity of ParvIR in the neuropil and an increase in the density of ParvIR neurons between P13 and P21. The pattern achieved by P21 persists into adulthood until at least P64. Thus, control rats from our sample have an age-appropriate distribution of ParvIR neurons in the cerebral cortex, similar to that reported previously.

Transient Effects of Neonatal Freeze Lesions

The decrease in density of ParvIR neurons within the microgyric regions in P13–P15 animals that had been apparent on casual examination of sections was confirmed with quantitative measures. In addition, a previously unappreciated decrease in ParvIR neuronal density in upper layers of regions located outside the area of the apparent malformation (PMZc and Dc) was found with quantitative measures. This decrease in superficial layers was not present in P21 or P64 animals, suggesting either a temporary down-regulation of parvalbumin immunoreactivity in microgyric cortex, or a delay in the maturation of ParvIR neurons. While data from the present experiment cannot distinguish between these two possibilities, there is evidence to support both ideas.

A temporary down-regulation could occur due to decreases in cortical activity. It has previously been demonstrated that parvalbumin and glutamic-acid decarboxylase (GAD) or GABA levels follow the level of afferent input to the cortex. For instance, decreases in sensory input to the cortex result in reduced immunocytochemical staining for parvalbumin and other GABA markers throughout the neocortical laminae (Hendry and Jones, 1986; Welker *et al.*, 1989b; Akhtar and Land, 1991; Micheva and Beaulieu, 1995; Carder *et al.*, 1996), while an increase in sensory drive can result in a more intense level of GAD immunoactivity (Welker *et al.*, 1989a). In the current study, the most severe decrease in activity levels would be expected within the microgyrus proper, due to loss of layers IV–VI and their normal afferents, and it is in this zone that the largest decrease in ParvIR neurons was found. Preliminary anatomical

findings demonstrating a near absence of thalamocortical input to the microgyria further support this idea (Rosen and Galaburda, 1998). The later increase in parvalbumin may reflect a return of activity levels due to formation of connections between neurons intrinsic to the microgyrus and other compensatory developmental processes.

A second explanation for temporary decreases in ParvIR is a delay in neuronal maturation. Previous work has demonstrated that radial glia fibers are retained into adulthood within the area of the microgyrus following freeze injury to the cortical plate at P1 (Rosen *et al.*, 1992). These results suggest a maintenance of the immature state, at least within the microgyrus itself. There may also be some delay in migration and subsequent differentiation, since the upper limiting membrane is typically damaged by the freeze lesion, and the radial glia fibers take some time to regrow (Rosen *et al.*, 1992). In addition, stabilization of otherwise developmentally transient projections follows the induction of microgyria in cats (Innocenti and Berbel, 1991a,b). Maintenance of an immature state has also been demonstrated after other types of neonatal lesions. For instance, tectal lesions combined with transplant of tectal tissue to the spinal cord results in the preservation of projections from the visual cortex to the spinal cord that are normally transient during development (Sharkey *et al.*, 1986). Also, lesions in rat ventroposterior thalamus at P7–P8 result in transient alterations in the relative expression of parvalbumin and calbindin in neocortical interneurons (Alcantara *et al.*, 1996b). There is a normal sequence for expression of calcium-binding proteins in some of these cells during the first three postnatal weeks involving shifts from calbindin, to calbindin plus parvalbumin, to parvalbumin alone (Alcantara *et al.*, 1993, 1996a). The thalamic lesion altered this sequence and caused a transient decrease in the number of parvalbumin-positive neurons and an increase numbers of calbindin-positive and parvalbumin-calbindin double-labeled neurons in neocortex (Alcantara *et al.*, 1996b). All three types of labeled neurons returned to control levels by the third postnatal week, suggesting a delay in maturation rather than a permanent reduction in parvalbumin expression.

Changes in neuronal ParvIR remote from the lesion (Fig. 5) may be secondary to the maturational delay seen within the microgyrus. For example, these remote neurons may not receive required chemical or electrophysiological signals from the adjacent damaged regions, leading to a delay in expression of parvalbumin. Development of parvalbumin expression is thought to depend on the establishment of physiological synaptic activity (Solbach and Celio, 1991). It is therefore possible that the temporary decrease seen in ParvIR neuron number results from a delay in the formation of cortical interconnections between the microgyral region and the adjacent paramicrogyral zone. Alternatively, the freeze lesion and subsequent reorganization of the cortex might result in the release of factor(s) that act to temporarily down-regulate the expression of parvalbumin in late-generated neurons.

Infragranular Effects of Neonatal Freeze Lesions in Older Animals

The large decrease in ParvIR cell number within stratum 3 of the microgyral column was not surprising, since there is a marked depletion of all neurons in this region due to the freeze lesion. However, the significant decrease in ParvIR numbers outside of the microgyrus was unexpected. This change was specific to layers IV and V in the area just adjacent to the microgyrus, with no change at sites 2 mm from the microgyrus. The spatial extent of changes in ParvIR is similar to the extent of cortex from which epileptiform activity can be evoked (Jacobs *et al.*, 1996a). While the functional effect of this decrease in parvalbumin has not been determined, a small concurrent reduction in releasable GABA in the same subset of neurons could contribute to the development of epileptiform potentials (e.g. a decrease in $GABA_A$-receptor inhibition of only 10–20% promotes the genesis and spread of epileptiform potentials within normal cortex) (Chagnac-Amitai and Connors, 1989; but see Jacobs *et al.*, 1996b).

There are a number of reports of anatomical abnormalities in the cortex surrounding the microgyrus, supporting the conclusion that aberrant development and reorganization occur in response to the loss of adjacent cortex. Glutamate immunocytochemistry has revealed disorganized axons in the paramicrogyral zone (Humphreys *et al.*, 1991), where increases in GFAP and neurofilament immunocytochemical staining also occur (K.M. Jacobs, I. Parada and D.A. Prince, unpublished observations; Humphreys *et al.*, 1991; Rosen *et al.*, 1992). Abnormalities in cytochrome oxidase and acetylcholinesterase staining adjacent to the microgyrus also suggest aberrant organization of thalamocortical afferents in this zone (Jacobs *et al.*, 1997). A similar reorganization of intracortical axons (e.g. Salin *et al.*, 1995), if present, might result in enhanced recurrent excitatory circuitry and thus provide another important mechanism for epileptogenesis (Prince and Connors, 1986; Wong *et al.*, 1986). The growth of most afferents into the cortex takes place in the microgyrus model after the lesion has occurred, thus suggesting that their aberrant organization is in response to the loss of adjacent cortical neurons rather than a direct effect of the lesion.

Widespread changes in cortical organization may arise as a result of the freeze lesion itself, or may be related to the more chronic effects of the malformed cortex on the remaining neocortex, such as epileptiform activity that may occur *in vivo* and propagate to remote cortical areas. Other types of lesions during development can result in abnormal connectivity that persists into adulthood. For example, in hamsters, neonatal lesions of the superior colliculus result in altered retinal projections (Finlay *et al.*, 1979; Schneider, 1979, 1981), and unilateral removal of facial whiskers in newborn rats results in the maintenance of a normally transient cross-modal projection between the medial geniculate nucleus of the thalamus and somatosensory cortex (Nicolelis *et al.*, 1991). Interhemispheric callosal connectivity can also be enhanced as a result of critically timed insults (Grigonis and Murphy, 1991; Miller *et al.*, 1993) and may be a feature of microgyria as well (Rosen *et al.*, 1989).

Summary and Conclusions

The density of ParvIR neurons was determined at different postnatal ages in neocortex from normal and microgyric rats. In normal cortex, as previously reported, ParvIR increased and assumed an adult pattern by P21. The induction of microgyria by a freeze lesion to the cortical plate at P0 or P1 caused both transient and more persistent effects on ParvIR in neurons of injured cortex. A transient decrease in the expression of ParvIR was found at P13–P15 in supragranular neurons both within the malformation itself and in six-layered cortex up to 2 mm adjacent to it, compared to control homotopic cortex. By P21, this difference in supragranular ParvIR neurons was no longer present. These results suggest that a delay in neuronal differentiation and synaptic maturation may occur in superficial laminae. The density of ParvIR neurons in laminae IV–VI was decreased

focally within and adjacent to the microgyrus, compared to controls at all ages studied (P13–P64). The spatial and temporal extent of effects in lower cortical laminae was consistent with previously reported epileptogenesis associated with microgyri in this model. Taken together, these results support previous research demonstrating widespread changes in cortical architecture as a result of early freeze injury to the cortical plate.

Notes

The authors wish to acknowledge the technical support of Alison Frank and Isabel Parada. This work was supported, in part, by grant HD 20806 from the Public Health Service of the USA and by NIH grants NS09806 and NS12151 from the NINDS.

Address correspondence to Glenn Rosen, Department of Neurology, Beth Israel Deaconess Medical Center, 330 Brookline Avenue, Boston, MA 02215, USA. Email: glenn_rosen@bidmc.harvard.edu.

References

Akhtar ND, Land PW (1991) Activity-dependent regulation of glutamic acid decarboxylase in the rat barrel cortex: effects of neonatal versus adult sensory deprivation. J Comp Neurol 307:200–213.

Alcantara S, Ferrer I, Soriano E (1993) Postnatal development of parvalbumin and calbindin d28K immunoreactivities in the cerebral cortex of the rat. Anat Embryol 188:63–73.

Alcantara S, de Lecea L, Del Rio JA, Ferrer I, Soriano E (1996a) Transient colocalization of parvalbumin and calbindin D28k in the postnatal cerebral cortex: evidence for a phenotypic shift in developing nonpyramidal neurons. Eur J Neurosci 8:1329–1339.

Alcantara S, Soriano E, Ferrer I (1996b) Thalamic and basal forebrain afferents modulate the development of parvalbumin and calbindin d28k immunoreactivity in the barrel cortex of the rat. Eur J Neurosci 8:1522–1534.

Carder RK, Leclerc SS, Hendry SH (1996) Regulation of calcium-binding protein immunoreactivity in GABA neurons of macaque primary visual cortex. Cereb Cortex 6:271–287.

Chagnac-Amitai Y, Connors BW (1989) Horizontal spread of synchronized activity in neocortex and its control by GABA-mediated inhibition. J Neurophysiol 61:747–758.

Denenberg VH (1979) Analysis of variance procedures for estimating reliability and comparing individual subjects. In: Origins of the infant's social responsiveness (Thoman E, ed.), pp. 339–348. Hillsdale, NJ: Erlbaum.

Dvorák K, Feit J (1977) Migration of neuroblasts through partial necrosis of the cerebral cortex in newborn rats — contribution to the problems of morphological development and developmental period of cerebral microgyria. Acta Neuropathol 38:203–212.

Dvorák K, Feit J, Juránková Z (1978) Experimentally induced focal microgyria and status verrucosus deformis in rats — Pathogenesis and interrelation histological and autoradiographical study. Acta Neuropathol 44:121–129.

Ferrer I, Pineda M, Tallada M, Oliver B, Russi A, Oller L, Noboa R, Zújar MJ, Alcántara S (1992) Abnormal local-circuit neurons in epilepsia partialis continua associated with focal cortical dysplasia. Acta Neuropathol 83:647–652.

Ferrer I, Alcántara S, Catala I, Zujar MJ (1993) Experimentally induced laminar necrosis, status verrucosus, focal cortical dysplasia reminiscent of microgyria, and porencephaly in the rat. Exp Brain Res 94:261–269.

Finlay BL, Wilson KG, Schneider GE (1979) Anomalous ipsilateral retinotectal projections in Syrian hamsters with early lesions: topography and functional capacity. J Comp Neurol 183:721–740.

Fitch RH, Tallal P, Brown C, Galaburda AM, Rosen GD (1994) Induced microgyria and auditory temporal processing in rats: A model for language impairment? Cereb Cortex 4:260–270.

Fitch RH, Brown CP, Tallal P, Rosen GD (1997) Effects of sex and MK-801 on auditory-processing deficits associated with developmental microgyric lesions in rats. Behav Neurosci 111:404–412.

Grigonis AM, Murphy EH (1991) Organization of callosal connections in the visual cortex of the rabbit following neonatal enucleation, dark rearing, and strobe rearing. J Comp Neurol 312:561–572.

Hendry SH, Jones EG (1986) Reduction in number of immunostained GABAergic neurones in deprived-eye dominance columns of monkey area 17. Nature 320:750–753.

Herman AE, Galaburda AM, Fitch HR, Carter AR, Rosen GD (1997) Cerebral microgyria, thalamic cell size and auditory temporal processing in male and female rats. Cereb Cortex 7:453–464.

Humphreys P, Rosen GD, Press DM, Sherman GF, Galaburda AM (1991) Freezing lesions of the newborn rat brain: a model for cerebrocortical microgyria. J Neuropathol Exp Neurol 50:145–160.

Innocenti GM, Berbel P (1991a) Analysis of an experimental cortical network: (i) architectonics of visual areas 17 and 18 after neonatal injections of ibotenic acid; similarities with human microgyria. J Neur Transplant 2:1–28.

Innocenti GM, Berbel P (1991b) Analysis of an experimental cortical network: (ii) connections of visual areas 17 and 18 after neonatal injections of ibotenic acid. J Neur Transplant 2:29–54.

Jacobs KM, Gutnick MJ, Prince DA (1996a) Hyperexcitability in a model of cortical maldevelopment. Cereb Cortex 6:514–523.

Jacobs KM, Huguenard JR, Prince DA (1996b) Inhibitory currents in a developmental model of epilepsy. Soc Neurosci Abstr 22:2102.

Jacobs KM, Mogensen M, Warren L, Prince DA (1997) Experimental microgyri disrupt cytochrome oxidase-identified barrel formation in rat somatosensory cortex. Soc Neurosci Abstr 23:811.

Luhmann HJ, Raabe K (1996) Characterization of neuronal migration disorders in neocortical structures. 1. Expression of epileptiform activity in an animal model. Epilepsy Res 26:67–74.

Luhmann HJ, Karpuk N, Qü M, Zilles K (1997) Neuronal migration disorders in rat cerebral cortex: electrophysiological and anatomical characterization. Soc Neurosci Abstr 23:807.

Marret S, Mukendi R, Gadisseux J, Gressens P, Evrard P (1995) Effect of ibotenate on brain development: an excitotoxic mouse model of microgyria and postthypoxic-like lesions. J Neuropathol Exp Neurol 54:358–370.

Micheva KD, Beaulieu C (1995) Neonatal sensory deprivation induces selective changes in the quantitative distribution of GABA-immunoreactive neurons in the rat barrel field cortex. J Comp Neurol 361:574–84.

Miller B, Nagy D, Finlay BL, Chance B, Kobayashi A, Nioka S (1993) Consequences of reduced cerebral blood flow in brain development. I. Gross morphology, histology, and callosal connectivity. Exp Neurol 124:326–342.

Nicolelis MAL, Chapin JK, Lin RCS (1991) Neonatal whisker removal in rats stabilizes a transient projection from the auditory thalamus to the primary somatosensory cortex. Brain Res 567:133–139.

Prince DA, Connors BW (1986) Mechanisms of interictal epileptogenesis. Adv Neurol 44:275–299.

Ren JQ, Aika Y, Heizmann CW, Kosaka T (1992) Quantitative analysis of neurons and glial cells in the rat somatosensory cortex, with special reference to GABAergic neurons and parvalbumin-containing neurons. Exp Brain Res 92:1–14.

Rosen GD, Galaburda AM (1998) Thalamocortical and corticothalamic connectivity in induced neocortical microgyria. Soc Neurosci Abstr 24:561.

Rosen GD, Galaburda AM, Sherman GF (1989) Cerebrocortical microdysgenesis with anomalous callosal connections: a case study in the rat. Int J Neurosci 47:237–247.

Rosen GD, Press DM, Sherman GF, Galaburda AM (1992) The development of induced cerebrocortical microgyria in the rat. J Neuropathol Exp Neurol 51:601–611.

Rosen GD, Sherman GF, Galaburda AM (1996) Birthdates of neurons in induced microgyria. Brain Res 727:71–78.

Salin P, Tseng GF, Hoffman S, Parada I, Prince DA (1995) Axonal sprouting in layer V pyramidal neurons of chronically injured cerebral cortex. J Neurosci 15:8234–245.

Sanchez MP, Frassoni C, Alvarez-Bolado G, Spreafico R, Fairen A (1992) Distribution of calbindin and parvalbumin in the developing somatosensory cortex and its primordium in the rat: an immunocytochemical study. J Neurocytol 21:717–736.

Schneider GE (1979) Is it really better to have your brain lesion early? A revision of the 'Kennard principle'. Neuropsychologia 17:557–583.

Schneider GE (1981) Early lesions and abnormal neuronal connections. Trends Neurosci 4:187–192.

Sharkey MA, Lund RD, Dom RM (1986) Maintenance of transient occipitospinal axons in the rat. Brain Res 395:257–261.

Solbach S, Celio MR (1991) Ontogeny of the calcium binding protein parvalbumin in the rat nervous system. Anat Embryol 184:103–124.

Soriano E, Del Rio JA, Ferrer I, Auladell C, De Lecea L, Alcantara S (1992) Late appearance of parvalbumin-immunoreactive neurons in the rodent cerebral cortex does not follow an inside-out sequence. Neurosci Lett 142:147–150.

Suzuki M, Choi BH (1991) Repair and reconstruction of the cortical plate following closed cryogenic injury to the neonatal rat cerebrum. Acta Neuropathol 82:93–101.

Welker E, Soriano E, Dorfl J, Van der Loos H (1989a) Plasticity in the barrel cortex of the adult mouse: transient increase of GAD-immunoreactivity following sensory stimulation. Exp Brain Res 78:659–664.

Welker E, Soriano E, Van der Loos H (1989b) Plasticity in the barrel cortex of the adult mouse: effects of peripheral deprivation on GAD-immunoreactivity. Exp Brain Res 74:441–452.

Williams RW, Rakic P (1988) Three-dimensional counting: an accurate and direct method to estimate numbers of cells in sectioned material. J Comp Neurol 278:344–352.

Wong RK, Traub RD, Miles R (1986) Cellular basis of neuronal synchrony in epilepsy. Adv Neurol 44:583–592.

Zilles K (1985) The cortex of the rat: a stereotaxic atlas. Berlin: Springer-Verlag.